HAL
open science

Modelling and Simulation of Acid Gas Condensation in an Industrial Chimney

Eric Serris, Michel Cournil, Peultier Jérôme

To cite this version:

Eric Serris, Michel Cournil, Peultier Jérôme. Modelling and Simulation of Acid Gas Condensation in an Industrial Chimney. International Journal of Chemical Reactor Engineering, 2009, pp.A39. 10.2202/1542-6580.1881 . hal-00495146

HAL Id: hal-00495146

https://hal.science/hal-00495146v1

Submitted on 30 Jun 2010

HAL is a multi-disciplinary open access archive for the deposit and dissemination of scientific research documents, whether they are published or not. The documents may come from teaching and research institutions in France or abroad, or from public or private research centers.

L'archive ouverte pluridisciplinaire **HAL**, est destinée au dépôt et à la diffusion de documents scientifiques de niveau recherche, publiés ou non, émanant des établissements d'enseignement et de recherche français ou étrangers, des laboratoires publics ou privés.

International Journal of Chemical Reactor Engineering, 2009, 7, A39
doi: 10.2202/1542-6580.1881

Modeling and simulation of acid gas condensation in an industrial chimney

ERIC SERRIS[(1)]*, MICHEL COURNIL[(2)], JÉRÔME PEULTIER[(3)]

[(1)] *Ecole Nationale Supérieure des Mines de Saint Etienne, Centre SPIN ; Département ProcESS ; LPMG UMR CNRS 5148 ; 158 Cours Fauriel ; 42023 Saint-Étienne Cedex 2, France*
[(2)] *Ecole Nationale Supérieure des Mines de Saint Etienne, Centre SPIN ; Département GENERIC ; LPMG UMR CNRS 5148 ; 158 Cours Fauriel ; 42023 Saint-Étienne Cedex 2, France*
[(3)] *INDUSTEEL, CRMC, Arcelor Group, 56 rue Clemenceau, BP 19, 71201 Le Creusot Cedex, France*

Abstract

Coal power stations as well as waste incinerators produce humid acid gases which may condense in industrial chimneys. These condensates can cause corrosion of chimney internal cladding which is made of stainless steel, nickel base alloys or non metallic materials. In the aim of polluting emission reduction and material optimal choice, it is necessary to determine and characterize all the phenomena which occur throughout the chimney and more especially condensation and dissolution of acid gases (in this particular case, sulfur dioxide SO_2).

Keywords:

modeling ; polluting emission ; mass and heat transfer ; industrial chimney ; acid gases

I. Introduction

Production of energy from fossil fuels (coal, oil, natural gas, etc.) gives rise to emission of gas which generally contains sulfur compounds (SO2, SO3) as well as chlorine and fluorine compounds. To avoid subsequent atmospheric pollution and its harmful effects (acid rains, impact on health) due to hydrochloric, sulfuric and hydrofluoric acids produced in the presence of air, it is necessary to steam these flue gases. Nevertheless, a considerable quantity of residual acid gases remains in the gas discharge which also contains large amount of water vapor. Thus, condensation may occur and by the way acid attack of the internal cladding of the chimney. This results in high maintenance costs and structural stability reduction.
Better knowledge of heat and mass transfer phenomena which accompany water condensation and dissolution of acid gases is necessary for more satisfactory design and rational material choice.
In this work we consider the following cases which are directly inspired by real installations:

- coal power station: the chimney of 250 m in height and 6.80 m in diameter is fed with a gas flow-rate of humid air (W_{air} = 2606300 m^3/hr or 2634200 kg/hr, W_{water} = 144300 kg/h *i.e.* 5.48%) which enters at temperature T_{gas} = 89 °C at the bottom.
- waste incinerator: the chimney of 100 m in height and 2.20 m in diameter is fed with a gas flow-rate of humid air (W_{air} = 173400 m^3/hr m^3/hr, W_{water} = 31210 m^3/h (18% of

* Corresponding author : serris@emse.fr

total flow) which enters at temperature T_{gas} = 67°C at the bottom. W_{air} = 173400 m^3/h; W_{water} = 31210 m^3/h (18% of total flow).

As we did not have a pilot installation at our disposal, we completed our study by indicative experiments using a vertical glass tube in which we could perform various systematic studies of condensation. Representativity of this set-up seems weak a priori; however we will prove its interest in the sequel especially for validating a model. This model, precisely, consists of a simplified, however realistic, representation of the different heat and mass transport phenomena in and around the chimney. Particular attention is given to local water condensation, formation and flow of a liquid layer and dissolution of acid gasses responsible for corrosion.

II. Modelling

In first part of this modelling section, we determine heat transfer in and around the chimney in presence of possible wall condensation phenomenon. Then, we take into account the dissolution of one of the major acid gases (SO_2) in the condensed phase. Geometrical configuration and main notation are shown in Figure 1.

II.1. Assumptions

Steady state conditions are supposed to be observed in the whole system. Cylindrical symmetry implies the use of vertical (z) and radial (r) coordinates; z-axis is oriented upwards.

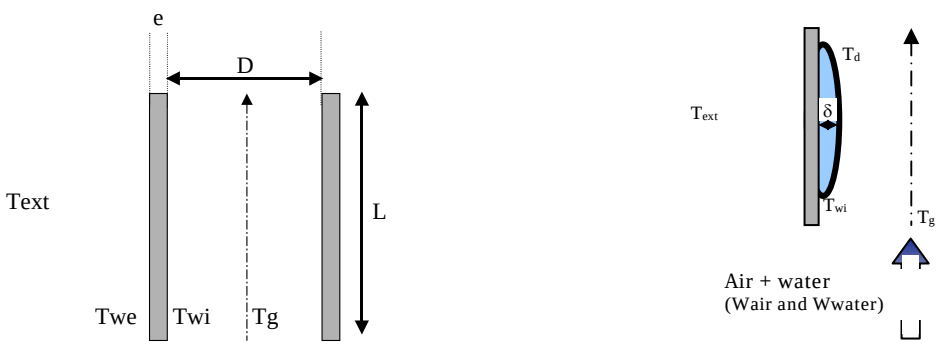

Figure 1: Chimney with and without condensation

R (resp. D) is the chimney internal radius (resp. diameter), L its total height and e the wall thickness. We consider the possibility that water vapour condenses along the wall giving a film in a limited area. The wall temperature is indeed too high downwards whereas air moisture is too low upwards. Liquid film thickness δ is assumed far smaller than the chimney radius.

We adopt a simplified description for the temperature distribution, that is to say, Tg, gas temperature on the chimney axis, Twi temperature on the internal wall and Twe on the external wall while Text is the outside temperature. Temperature profile is assumed linear in the wall thickness as well in the liquid film layer according to the Fourier's law. We call v the average drainage velocity of the water film, δ its thickness and Td the surface temperature of this flowing film. Td corresponds to the condensation temperature of the water vapor at local conditions of the chimney. This latter assumption was already applied by Nussel in [1].

II.2. Equations

Water mass balance written on a slice of chimney of thickness dz expresses as:

$$\frac{dW_{water}}{dz} = \frac{-2W_{cond}}{R} \tag{1}$$

Wwater and Wcond are respectively the mass flow-rate of water vapour and the condensation flow-rate.

Global water mass balance considered for both liquid and gas phases between height zero and z is expressed as:

$$2\rho_{water} v\delta(z) = R(W_{water}(z) - W_{water}(0)) \tag{2}$$

ρwater is the density of liquid water.
Liquid film velocity and thickness are linked by the well-known relation [2].

$$v = \frac{\rho_{water} g\delta^2}{3\mu_{water}} \tag{3}$$

Heat balance written respectively in liquid and gas phase expresses as:

$$2W_{cond} - 2H(T_{wi} - T_{ext}) + h_{\text{int}}(T_g - T_d) = 0 \tag{4}$$

$$\frac{dT_g}{dz} = \frac{-h_{\text{int}}(T_g - T_d)}{R(C_{p_{water}} W_{water} + C_{p_{air}} W_{air})} \tag{5}$$

H the coefficient of global heat transfer defined by the relation:

$$\frac{1}{\text{H}} = \frac{1}{h_{ext}} + \frac{e}{k_w} \tag{6}$$

where kw is the wall heat conductivity, h_{int} and h_{ext} are the respectively heat transfer coefficients inside and outside the chimney
A last equation is obtained from the continuity condition of the conductive heat flux in the wall and in the liquid film:

$$T_{wi} = \left(\frac{1}{1 + \frac{\delta H}{K_{water}}}\right) T_d + \left(H + \frac{\delta}{H\delta + K_{water}}\right) T_{ext} \tag{7}$$

Kwater is the water thermal conductivity.

Heat transfer coefficients are obtained from correlations:
to determine h_{ext}, we use a usual correlation for perpendicular flow turbulent (wind) to the axis of the chimney [3].

$$\text{Nu} = 0.023\text{Re}^{4/5}\text{Pr}^{2/5} = \frac{h_{ext}(D + 2e)}{k} \tag{8}$$

Hence the following expression of hext is obtained:

$$h_{ext} = 0.023\frac{k(T_{ext})}{(D + 2e)}\text{Re}^{\frac{4}{5}}\text{Pr}^{\frac{2}{5}} = 0.023\frac{k(T_{ext})}{(D + 2e)}\left(\frac{v_{wind}(D + 2e)}{\nu(T_{ext})}\right)^{\frac{4}{5}}\left(\frac{\nu(T_{ext})}{\alpha(T_{ext})}\right)^{\frac{2}{5}} \tag{9}$$

vwind is the wind velocity outside the chimney.
with k(T) thermal conductivity, ν(T) kinematic viscosity and α(T) thermal diffusivity of air at temperature T.
Inside the chimney Reynolds number is high (Re > 104), thus we apply the following correlation suitable for inner heat transfer from turbulent flows in cylindrical tubes [4]:

$$\mathrm{Nu} = 0.023\mathrm{Re}^{\frac{4}{5}}\mathrm{Pr}^{\frac{1}{3}} = \frac{h_{\mathrm{int}}D}{k} \tag{10}$$

Hence:

$$h_{\mathrm{int}} = 0.023\frac{k(T_g)}{D}\mathrm{Re}^{\frac{4}{5}}\mathrm{Pr}^{\frac{1}{3}} = 0.023\frac{k(T_g)}{D}\left(\frac{4W_{air}D}{\pi D^2\nu(T_g)}\right)^{\frac{4}{5}}\left(\frac{\nu(T_g)}{\alpha(T_g)}\right)^{\frac{1}{3}} \tag{11}$$

Reaction of absorption of sulfur dioxide gas into water is as follows:

$H_2O + SO_2 = H_2SO_3$

In this work, we suppose it very rapid so that equilibrium is instantaneously reached. This assumption allows us to determine the lowest pH value in the liquid film, *i.e.*, the worst conditions as regards the acidity and its consequences on corrosion.
Sulfurous acid concentration (H_2SO_3) can be thus expressed as a function of partial pressure of sulfur dioxide (SO_2) according to:

$$K(T) = \frac{[\mathrm{H_2SO_3}]}{\mathrm{P_{SO_2}}} \tag{12}$$

Solubility constant K (T) is deduced from the literature data [5] (K(T) = 7.18 exp-(0.0341T). In present conditions, only first acidity of sulfurous acid (Ka1) is to be taken into account. By expressing the sulfurous acid concentration, the pH value is obtained as a function of temperature and sulfur dioxide partial pressure:

$$\mathrm{pH} = -\ln\left(\frac{-K_{a1} + \sqrt{K_{a1}^2 + 4K_{a1}7.18\exp(-0.0341\,T)P_{\mathrm{SO_2}}}}{2}\right) \tag{13}$$

Starting from Equations (1) and (5) and taking into account previous relations between variables, numerical values of the different flow-rates, temperature, concentrations and δ (if need be) can be calculated as a function of z thanks to ordinary differential equations solvers.

III. Model application to real cases

The previous model is now applied to the two real cases presented in the introduction of this work.
We comment on only typical situations.

III.1. Coal power station

Main parameter values have been indicated above.

- for an external temperature of 25°C and a wind velocity 10 m.s^{-1} which are often considered as nominal conditions, condensation is not observed on the wall of the 225 m chimney;
- in fact, condensation would require higher content in water, lower external temperature and more efficient heat transfer; to simulate these conditions we chose a water flow-rate corresponding to 10 % of the total flow-rate, wind velocity outside the chimney equal to 22 m.s^{-1} and outside temperature of 0°C.

The flowing film of condensed water is indeed formed above approximately 100 meters height.
The results obtained in this case are shown in Figures 2 and 3. Figures 2(a) and 2(b) represent the temperatures of the gas and the internal wall in the “dry” wall area (a) and in the liquid film area (b) as a function of the height in the chimney. Figures 3(c) and 3(b) show

respectively the thickness of the flowing film and its pH value as a function of the height in the chimney.

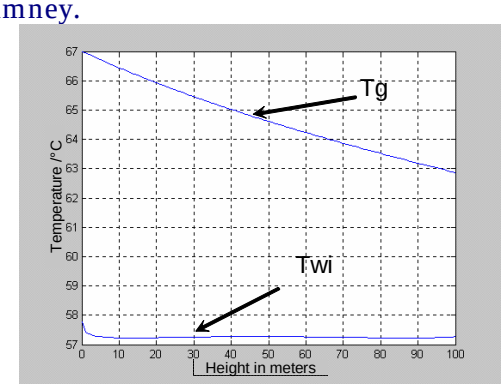

(a)

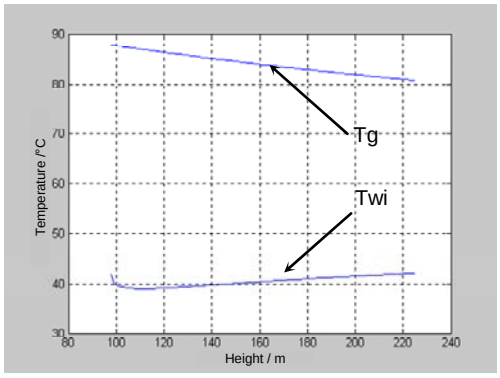

(b)

Figure 2: Variation of gas temperature of the wall below (a) and in (b) the condensation area

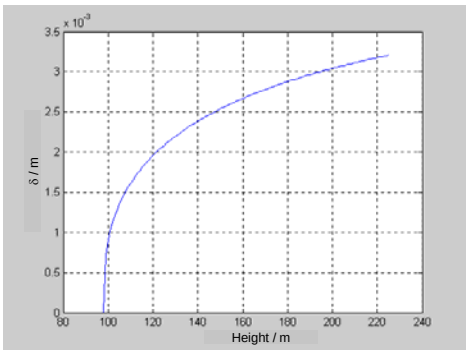

(c)

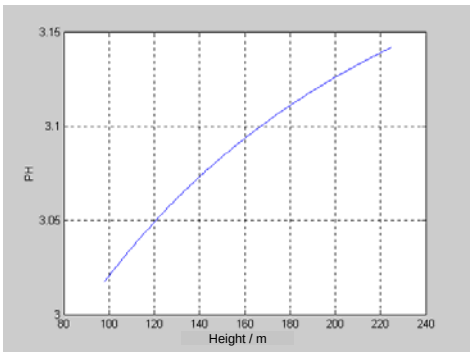

(d)

Figure 3: Liquid film thickness (c) and pH (d) along the chimney

We can notice that the temperature of the gas at the top of the chimney does not drop much with respect to the initial temperature. Furthermore, we notice that the flowing film thickness does not exceed a few millimeters and that its pH is relatively low (pH ~3) and constant. These results confirm that corrosion can be expected only in the upper part of the chimney and certainly occurs because of the temperature and pH values.

III.2. Waste incinerators

We adopt the same nominal external conditions as previously, *i.e.* T_{ext} = 25°C and v_{wind}= 10 m.s^{-1}. Figure 4(a) represents the evolution of gas temperature and wall temperature versus height in the chimney. Figure 4(b) (resp. 4(c)) shows the thickness of the water film (resp. pH) versus height in the chimney.

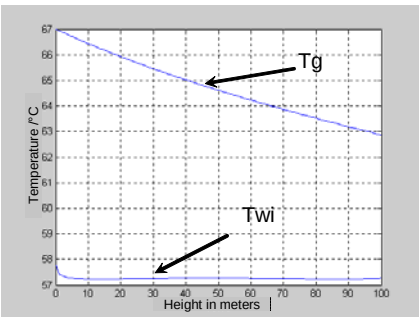

(a)

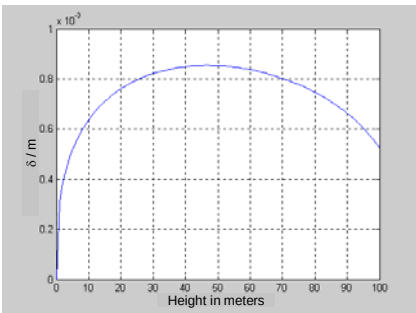

(b)

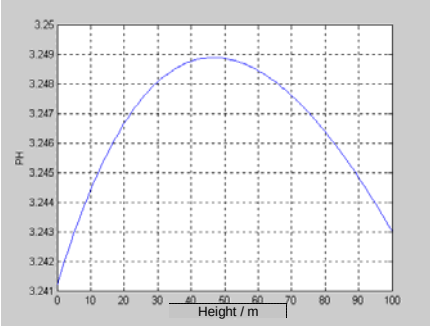

(c)

Figure 4: Variation of gas and wall temperature (a) liquid film thickness (b) and pH (c) versus height in the chimney

In this example, we observe that the liquid film flows along the whole height of the chimney. We observe again moderate variations of the different temperatures. The flowing film is thinner than previously and the calculated pH (again about 3) is almost constant.

For lower wind speed, however, condensation would not take place on all the height of the chimney. For example with an external wind of 2 m.s^{-1} condensation occurs above 60 m only.

This first application of our model proves that condensation and consequently corrosion does not necessarily concern the whole height of the chimney. This means that a part of the chimney only requires then a corrosion resistant steel cladding, for the rest of a less noble and cheaper material should be sufficient.

We are aware that some of the model elements are questionable and more especially the correlation choice for expressing the heat transfer coefficients. Coefficients h_{int} and H seem fairly reliable. We can note anyway that the global characteristics of the chimney, in particular as regards the onset and the location of condensation, are strongly sensitive to the external conditions (wind velocity and temperature) via h_{ext}. Expression of h_{int}, however, is more doubtful, especially in presence of a condensing flowing liquid film which is generally considered as an accelerating factor for heat transfer. This means that in our model, h_{int}, is probably underestimated. Consequences of this imprecision are not serious, insofar as internal heat transfer is rapid compared to external heat transfer. Another more delicate problem concerns the formation, nature and behavior of the condensed film. In our model we assume that condensation takes place as soon as supersaturation is ensured in the vapor phase, that is to say, we neglect a possible condensation delay due to nucleation. More generally we consider that mass-transfer is not rate-determining. We consider also that a continuous liquid film is immediately formed whereas in the reality isolated droplets should be observed in the upper zone of the condensation area. Due to gravity, however, a continuous film should appear in the lower zone particularly in case of notable condensation in consistency with our model.

IV. Experimental part

As aforesaid, the present experimental part does not claim to be as exhaustive as a systematic study on a pilot chimney, but is rather intended to emphasize different aspects of the condensation process and to confirm or not the assumptions of the previous model.

IV.1. Experimental set-up

We tried to design and operate a set-up which could allow us to observe water condensation in a long tube for various experimental conditions. Its schematic representation is shown in Figure 5.

A three neck flask of water maintained at fixed temperature and provided with air flow bubbling allows us to ensure relative humidity corresponding to the industrial conditions. The so produced wet gas is preheated in a tube surrounded with heating cords and then pumped into another three neck flask also surrounded with heating cords. A long glass tube mimics the industrial chimney by allowing water condensation and giving also the possibility of

qualitative and quantitative observation of the process. At the set-up upper part, the gas is passed to a cooling tube in order to condense the rest of water vapor which is collected. Outlet temperature of the gas is measured in this point. In Figure 5 are indicated also three measurement points (T_{p1}, T_{p2} and T_{p3}) of the wall temperature. After streaming along the tube, water is pumped up by a peristaltic pump and collected in a beaker. Percentage of condensed water is noted %C.R in the follow-up.

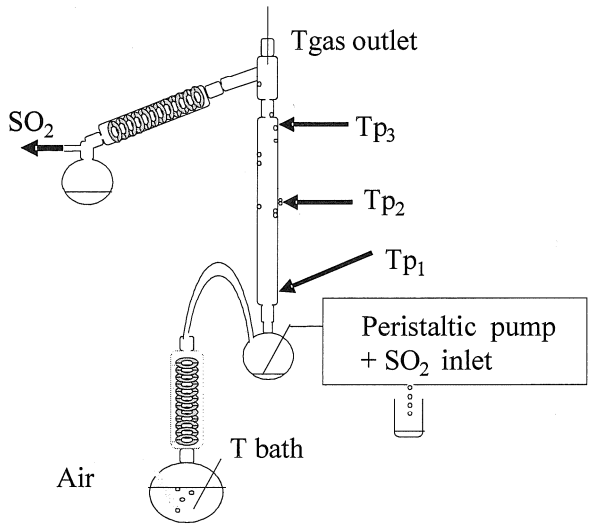

Figure 5: Experimental set-up

IV.2. Influence of gas humidity

Thanks to our experimental set-up, flask temperature can be fixed to vary the moisture content W_{water} of the in-going gas stream between 10% and 20% (total flow: 300 N L.hr^{-1}) Initial input gas temperature can be varied from 65°C up to 90°C. Figure 6 shows the variation of the outgoing gas stream temperature, the wall temperature at the tube lower part T_{p1} and of ratio %C.R. at different temperature values of the in-going gas.

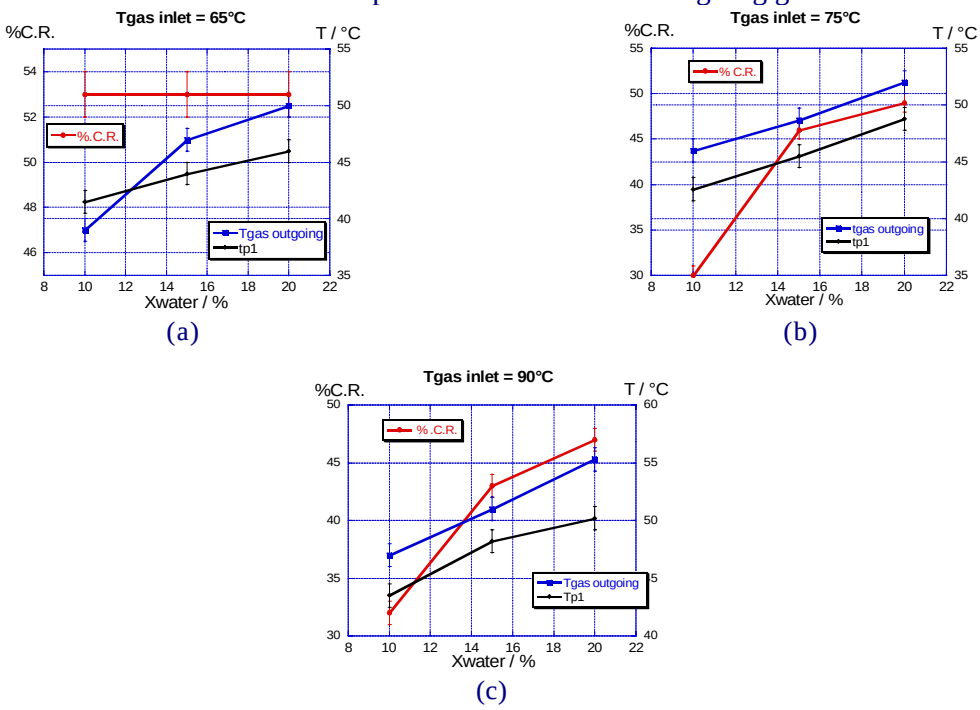

Figure 6: Influence of gas humidity

In each case (fig 6a, 6b, 6c), wall temperature Tp_1 increases when moisture content x_{water} increases. It is qualitatively consistent with model Equation (7) which gives the wall temperature as a function of film temperature T_d and external temperature T_{ext}. In chimney, temperature T_{wi} is thus increasing as a function of temperature T_d which corresponds (in our column) to the temperature of the flask which generates the water vapor. When this temperature increases it has the effect of increasing the internal wall temperature and thus the external wall as well as x_{water}.
We also note a constant increase of T_g with x_{water}. in Figures 6(a), 6(b) and 6(c). If we come back to relation (5) which describes the evolution of T_g, we can notice that an increase in T_d (or equivalently x_{water}) causes the decrease of the absolute value of the derivative of T_g versus z. As a consequence, the outgoing gas temperature of the chimney increases.
We observe an increase of %C.R when increasing x_{water} in Figures 6(b) and 6(c) excepted for the lowest gas temperature in Figure 6(a). Equation (4) shows that when T_d increases, W_{cond} increases.
At gas temperature of 65°C, however, we note that % .C.R is constant and thus x_{water} has no influence on the condensation contrarily to what is expected according to our model. At the moment we have no clear explanation of this result.

IV.3. Experiments with acid gas: SO_2

Sulfur dioxide is not introduced at the beginning of the experiment which starts as previously until condensation of water is obtained on the tube wall. Then sulfur dioxide is introduced (200 ppm of SO_2 dilute in air) as shown in Figure 5. Experiments involving SO_2 are 90 min long.
Condensed water which is recovered at the top and the bottom of the column can be then characterized. A DIONEX ionic chromatography apparatus is used as main analysis technique.
An example of chromatogram of both solutions collected at the top and at the bottom of column is presented in Figure 7.

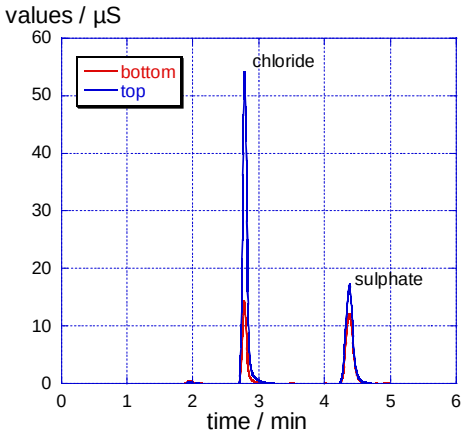

Figure 7: Collected water condensate chromatograms

The presence of chlorides on chromatograms is simply due to pollution of beakers. It should not be taken into account. We also detect sulfate ions instead of expected sulfites because the chromatography analysis is performed 24 hours after the tests. During this time sulfite ions react with oxygen to give sulfate ions. We can determine the concentration in sulfate ion thanks to standardization performed with solutions of known concentrations. For example, results from three different experiments are shown in Table 1.
Experiments 1 and 2 are intended to test the reproducibility of our experiments. This reproducibility is quite good, given that we do not control the quantity of condensed water in the flowing film on the walls before the introduction of SO_2. Indeed, we note the same quantity of water at the top and at the bottom of the column with similar pH and concentration in sulfate ions.

Table 1: Concentrations top and bottom

n° exp	parameters		collected water mass(g)	$[SO_4^{2-}]$	Measured pH
1	300 NL.h-1; T_{gas} = 75 °C, 200 ppm SO_2 10 % water	top	10.2	15.6 $g.L^{-1}$	3.55
		bottom	14.8	13.0 $g.L^{-1}$	3.55
2	300 NL.h-1; T_{gas} = 75 °C, 200 ppm SO_2 10 % water	top	12.0	14.5 $g.L^{-1}$	3.52
		bottom	18.6	10.2 $g.L^{-1}$	3.73
3	300 NL.h-1; T_{gas} = 105 °C, 200 ppm SO_2 10 % water	top	14.0	5.6 $g.L^{-1}$	4
		bottom	9.8	10.9 $g.L^{-1}$	3.73

If we compare now experiments 2 and 3, we note that they only differ in the temperature of the entering gas. We collect less water at the bottom of the chimney than previously thus we have less condensation as we observed in experiments 1 and 2. Furthermore, concentration in sulfate ions at the bottom of the column for all three experiments is the same, even although twice more water is obtained in experiment 3. This confirms that SO_2 absorption only depends on the temperature of water condensed on the wall. This temperature is fixed by the temperature of the lower three neck flask which does not change in both experiments. This is consistent with the assumption of thermodynamic equilibrium which was taken in our model.
Although measured pH values are relative to solutions of sulfate ions, they are practically equal to the original pH values in the sulfite ion solution which is collected during the experiment. They are close to the pH values calculated by our column model (Figures 3(d) and 4(c)).

V. Conclusions

In this work we propose different approach angles to the condensation phenomenon of acid gases in industrial chimneys. Understanding and prediction of this phenomenon is particularly useful for the choice of cladding materials liable to resist to corrosion. The model we propose takes into account in a simple however realistic way the different heat and mass transfer phenomena. Condensation process is considered at the equilibrium. Nucleation is not a relevant step. Thanks to this model, it is easy to obtain a good approximation of the main parameters of the system for given experimental conditions:

- existence and location of the condensation zone;
- thickness and acidity of the condensed film.

In the absence of a pilot installation, a laboratory column allows us to validate the influence of parameters such as input gas temperature, gas flow-rate and water percentage in gas.
The model we develop reveals a fair consistency with the experimental observations which provide us with interesting tracks to refine it. In the reality as well as in the model, the most important parameters are in fact internal and external heat transfer coefficients which govern the main thermal processes. External heat transfer coefficient is above all determined by the weather conditions thus it is hardly controllable and can be considered as imposed. As for the internal heat coefficient, it is relatively sensitive to internal gas velocity and correlations which allow its calculation have a questionable reliability. Thus an experimental identification on installation or on pilot plan should be imperative. Concerning pH of the flowing film of condensed water, experiments show that SO_2dissolution is rather fast and that flowing film acidity is high even in presence of a small amount of SO_2.
In spite of its simplicity, present study offers nevertheless an interest to predict qualitatively and quantitatively the main phenomena (condensation) and the essential characteristics (zone of condensation, pH) in an industrial chimney.

References

[1] Nusselt, W.:Die Oberflächenkondensation des Wasserdampfes, VDI-Z. 60 (1916), p541-546, 569-575.
[2] Bird,R.B., Stewart, W.E., Lightfoot, E.N., Transport Phenomena, 2nd Edition, John Wiley & Sons, 2002, New York.
[3] Žukauskas, A.A..; Žingžda,J.: Heat transfert of a cylinder in cross flow. Washington: Hemisphere Publ. Comp. (1986), p162
[4] Mc-Adams, W.: Heat transmission 2nd edition, New-York: McGraw Hill (1942) p 168.
[5] Hackspill L, Besson J, Herold A, Chimie générale, Paris, Presses universitaires de France (1964) p 416